AD_____

GRANT NO: DAMD17-93-J-3066

TITLE: Genotoxic Assessment of DNA and Cellular Fractions from Cancerous Tissues: A Prognostic Assay for Cancer Risk

PRINCIPAL INVESTIGATOR: Donald C. Malins, Ph.D., D.Sc.

CONTRACTING ORGANIZATION: Pacific Northwest Research Foundation
720 Broadway
Seattle, Washington 98122

REPORT DATE: December 29, 1994

TYPE OF REPORT: Final Report

PREPARED FOR: U.S. Army Medical Research and Materiel Command
Fort Detrick
Frederick, Maryland 21702-5012

DISTRIBUTION STATEMENT: Approved for public release; distribution unlimited

REPORT DOCUMENTATION PAGE

Form Approved
OMB No. 0704-0188

1. AGENCY USE ONLY (Leave blank)	2. REPORT DATE	3. REPORT TYPE AND DATES COVERED
	29 Dec 94	Final 1 Sept 93 - 30 Nov 94

4. TITLE AND SUBTITLE
Genotoxic Assessment of DNA and Cellular Fractions from Cancerous Tissues: A Prognostic Assay for Cancer Risk

5. FUNDING NUMBERS
DAMD17-93-J-3066

6. AUTHOR(S)
Donald C. Malins, Ph.D., D.Sc.

7. PERFORMING ORGANIZATION NAME(S) AND ADDRESS(ES)
Pacific Northwest Research Foundation
720 Broadway
Seattle, Washington 98122

8. PERFORMING ORGANIZATION REPORT NUMBER

9. SPONSORING / MONITORING AGENCY NAME(S) AND ADDRESS(ES)
U.S. Army Medical Research and Materiel Command
Fort Detrick, Frederick, MD 21702-5012

10. SPONSORING / MONITORING AGENCY REPORT NUMBER

11. SUPPLEMENTARY NOTES

12a. DISTRIBUTION / AVAILABILITY STATEMENT
Approved for public release, distribution unlimited

12b. DISTRIBUTION CODE

13. ABSTRACT *(Maximum 200 words)*

14. SUBJECT TERMS
Fish, Molecular Biology

15. NUMBER OF PAGES
42

16. PRICE CODE

17. SECURITY CLASSIFICATION OF REPORT	18. SECURITY CLASSIFICATION OF THIS PAGE	19. SECURITY CLASSIFICATION OF ABSTRACT	20. LIMITATION OF ABSTRACT
Unclassified	Unclassified	Unclassified	Unlimited

FOREWORD

Opinions, interpretations, conclusions and recommendations are those of the author and are not necessarily endorsed by the US Army.

✓ Where copyrighted material is quoted, permission has been obtained to use such material.

✓ Where material from documents designated for limited distribution is quoted, permission has been obtained to use the material.

✓ Citations of commercial organizations and trade names in this report do not constitute an official Department of Army endorsement or approval of the products or services of these organizations.

✓ In conducting research using animals, the investigator(s) adhered to the "Guide for the Care and Use of Laboratory Animals," prepared by the Committee on Care and Use of Laboratory Animals of the Institute of Laboratory Resources, National Research Council (NIH Publication No. 86-23, Revised 1985).

✓ For the protection of human subjects, the investigator(s) adhered to policies of applicable Federal Law 45 CFR 46.

NA In conducting research utilizing recombinant DNA technology, the investigator(s) adhered to current guidelines promulgated by the National Institutes of Health.

NA In the conduct of research utilizing recombinant DNA, the investigator(s) adhered to the NIH Guidelines for Research Involving Recombinant DNA Molecules.

NA In the conduct of research involving hazardous organisms, the investigator(s) adhered to the CDC-NIH Guide for Biosafety in Microbiological and Biomedical Laboratories.

Accesion For	
NTIS CRA&I	☒
DTIC TAB	☐
Unannounced	☐
Justification	
By	
Distribution /	
Availability Codes	
Dist	Avail and / or Special
A-1	

PI - Signature Date

TABLE OF CONTENTS

I. INTRODUCTION

A. Nature of the Problem

Factors that elicit mutagenic damage to the DNA have been intensely studied for over 50 years. These reactions include the introduction of bulky substituents on the DNA bases which are products of two-electron oxidations (1). Recent studies on these DNA changes suggest that they are more prone to blocking DNA replication and transcription than creating mutagenic lesions (2). A second means of creating potentially mutagenic changes to the DNA is through one-electron, radical-induced oxidative modifications of the nucleotide bases (3). One such free radical is the hydroxyl radical, •OH. The •OH is likely generated *in vivo* from H_2O_2 in a Fe^{++}-catalyzed Fenton reaction (4, 5). The source of H_2O_2 may be through cytochrome P-450 oxidoreductase cycling after exposure of the tissue to various types of endogenous and exogenous chemicals (6). In fact, those chemicals capable of forming bulky adducts with DNA through two-electron oxidations also form one or more moles of H_2O_2 per mole of bulky adduct. Thus, both processes occur simultaneously. Historically, it has been routinely possible to identify and measure the incidence of the bulky adducts by means of techniques such as ^{32}P-postlabeling analysis (7). These experiments have defined the concentrations of such lesions to be in the 1 in 10^7 to 1 in 10^9 range. The •OH damage in DNA of living tissues has, until very recently, been virtually impossible to measure due to the need to identify subtle changes in the molecule, such as the addition of a single O atom (e.g., in the formation of 8-OH-guanine [8-OH-Gua] from guanine). Our work fills this gap in knowledge by showing that

radical-induced DNA lesions are dramatically higher in concentration in both histologically normal and neoplastic tissues, often representing one modification in several hundred bases (8-13).

The following are among the problems remaining. There is a need to obtain a more comprehensive understanding of the nature and distribution of the base lesions among different phyla and tissues and determine whether other aspects of the DNA molecule are altered in relation to carcinogenesis. There is also a need to establish statistical (predictive) models. The work undertaken in the one-year period of the present study resulted in progress toward addressing these important issues.

B. Background of previous work

Several •OH-induced base lesions have been reported in the literature; however, these studies were primarily conducted with *in vitro* systems (14). Their presence in tissue and their connection to carcinogenesis *in vivo* was described for the first time in reports from our laboratory (8-13). For example, the purine rings of both adenine and guanine undergo two types of radical-induced modifications *in vivo*--ring opening reactions forming Fapy derivatives and hydroxylation reactions yielding 8-OH adducts. The 8-OH adduction products (e.g., 8-OH-Gua) have been shown to be mutagenic because of their 1- to 2% level of misrepair during DNA replication leading, for example, to G→T transversions (15). In contrast, Fapy derivatives appear to be essentially non-mutagenic due to their strong ability to block DNA replication until they are repaired (2). Thus,

•OH-induced DNA reaction products are especially important contributors to the carcinogenic potential induced by chemical stimuli, to include hormone derivatives (e.g., estrogen) and exogenous chemicals (e.g., PCBs and DDT).

Specifically, in our initial study of DNA base lesions in biological systems, using gas-chromatography-mass spectrometry with selected ion monitoring (GC-MS/SIM), a relatively high concentration of the ring-opening product of guanine (2,6-diamino-4-hydroxy-5-formamidopyrimidine; Fapy-G) was found in hepatic tumors of English sole exposed to environmental carcinogens. This was the first time that a ring-opening base lesion had been found in a living system (8). We also found that Medaka exposed to environmental chemicals (e.g., from ground water) at Fort Detrick developed elevated levels of the base lesions in the liver. These base lesions returned to essentially normal levels after the fish were placed in clean water, suggesting that the DNA base damage is reversible when the chemical stress is terminated.

Later the English sole neoplasms were shown to contain a high concentration of the ring-opening product of adenine (4,6-diamino-5-formamidopyrimidine; Fapy-A), as well as 8-OH-Gua and 8-OH-adenine (8-OH-Ade) (9, Figure 1). Ring-opening products are formed primarily via reductive pathways from the respective 8-oxyl derivatives, whereas the OH-adducts are formed oxidatively from the same precursors (12). The 8-OH-Gua lesion has been variously implicated as a mutagen and carcinogen (14) and, importantly, has been shown to have an overwhelming effect in causing misreplication in template-directed DNA synthesis (15).

Figure 1. ***Purine base lesions studied***

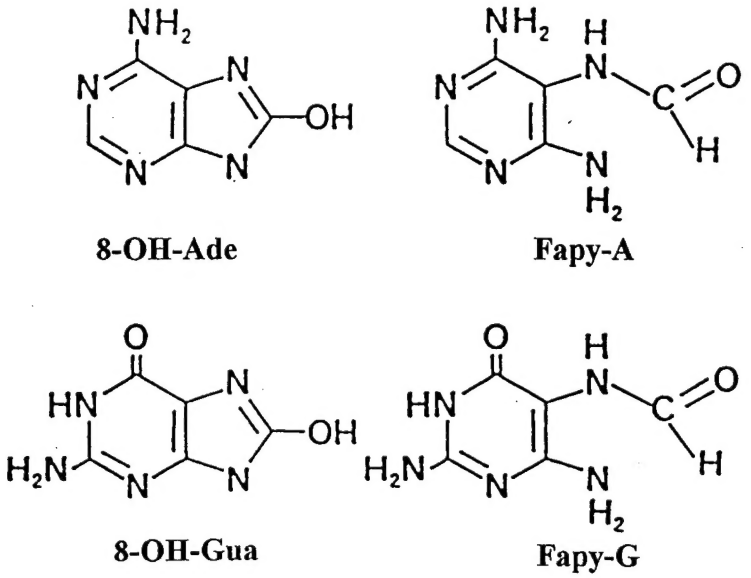

Initial evidence (8, 9) suggested that the DNA base lesions may be sensitive and convenient biomarkers for cancer risk assessment. This potential was enhanced when the base lesions were found in microscopically normal livers of English sole living in a moderately polluted environment in which the incidence of hepatic cancer among the fish population was found to be less than 5% (11). The liver of normal fish from essentially clean environments had comparatively very low DNA base lesion concentrations.

In a subsequent experiment, evidence was found for the first time for elevated concentrations of purine base lesions in a mammalian tissue--the cancerous female breast (10). The degree of damage to the DNA base structure was generally remarkably high (frequently representing one base lesion in several hundred normal bases), as was the case with the neoplastic hepatic tissues of the fish. Thus, at this point, evidence with diverse

biological systems suggested that the base lesions play a significant role in the etiology of cancer in phylogenetically diverse species and are potentially useful biomarkers for estimating cancer risk on the basis of predictive models.

A variety of other base lesions were later identified in other cancers. These additional base lesions included 5-hydroxycytosine and 5-hydroxhydantoin from the human brain, lung and other human tissues (16).

Specifically, the most recent studies from our laboratory, focusing on DNA isolated from normal female breast tissue (reduction mammoplasty tissue; RMT), as well as invasive ductal carcinoma (IDC) and microscopically normal tissue (MNT) from non-neoplastic regions of the cancerous breast, have provided extensive insight into the biological relevance of •OH-induced base lesions in oncogenesis. These results, based on 22 statistical models of the reductively and oxidatively-formed base lesions (Table 1; a number having a sensitivity and specificity of 90-97%*), were published recently in Cancer (12), coupled with a supportive editorial by Dr. S. Thorgeirsson (17), head of the Chemical Carcinogenesis Branch of the NCI.

The research indicated that both normal and cancerous breast tissues are under substantial oxidative stress which, most significantly, is translated into different types of base lesion profiles. Normal tissue was characterized by substantial elevations of ring-opening Fapy derivatives over 8-OH adducts by a factor of from three to ten fold. In contrast, both tumor and microscopically normal tissue from cancer patients had essentially the inverse relationship of these base lesions.

---

* Sensitivity is the percentage of cancer tissue samples that were correctly classified (true-positives) using the models, and specificity is the percentage of non-cancer tissue samples that were correctly classified (true-negatives).

Table 1. ***Mean log_{10} concentrations and log_{10} ratios of concentrations of DNA-base lesions from reductive mammoplasty tissue (RMT) and cancerous breast tissue (IDC and MNT) and sensitivity and specificity based on statistical models.****

Indicator		Non-cancer patients		Cancer patients		Predictive Model (Logistic regression)		
log_{10} (concentrations)	P-value†	Mean§	S.E.	Mean§	S.E.	Sensitivity (%)	Specificity (%)	P-value‡
HMUra	.0000	-3.3	.1	-2.8	.1	91	69	.0001
Fapy-A	.0000	.2	.1	-.7	.1	82	93	.0000
log_{10} (ratio of concentrations)								
Fapy-A/HMUra	.0000	3.6	.1	2.0	.1	91	97	.0001
Fapy-A-8/OH-Ade	.0000	.9	.1	-.3	.1	91	96	.0000
Fapy-A/8-OH-Gua	.0000	1.4	.1	.2	.1	91	94	.0001
Fapy-A/(8-OH-Ade + 8-OH-Gua)	.0000	.8	.1	-.4	.1	91	97	.0001
Fapy-A/(8-OH-Ade + 8-OH-Gua + HMUra)	.0000	.8	.1	-.4	.1	91	97	.0001
(Fapy-A + Fapy-G)/ (8-OH-Ade + 8-OH-Gua)	.0000	.8	.1	-.4	.1	91	97	.0000
(Fapy-A + Fapy-G)/ (8-OH-Ade + 8-OH-Gua + HMUra)	.0000	.8	.1	-.4	.1	91	97	.0000

*All analyses are based on n = 15 cancer patients with a total of 22 tissue samples and 15 non-cancer patients with a total of 70 tissue samples.

†Based on linear regression random-effects model, testing the null hypothesis of equality of means for cancer and non-cancer (RMT) patients.

§Mean of the log_{10} values for the tissue specimens.

‡Based on logistic regression random-effects model, testing the null hypothesis that the log_{10} value is not associated with cancer vs. non-cancer (RMT) classification of tissue section.

Table 2 shows the use of two of the base lesion models to allow for the classification of cancer vs. non-cancer with correct classifications being about 95%.

Table 2. ***Classification of tissue sections using predictive model based on ratio of concentrations: (Fapy-A + Fapy-G)/(8-OH-Ade + 8-OH-Gua) or (Fapy-A)/(8-OH-Gua)*.***

Patient #, type of patient	Classification of sections based on (Fapy-A + Fapy-G/(8-OH-Ade + 8-OH-Gua + HMUra) N incorrect/N total	Classification of sections based on (Fapy-A)/(8-OH-Gua) N incorrect/N total
1, RM	0/7	0/7
2, RM	0/13	2/13
3, RM	0/4	1/4
4, RM	0/5	1/5
5, RM	1/5	0/5
6, RM	0/5	0/5
7, RM	0/5	0/5
8, RM	0/6	0/6
9, RM	0/5	0/5
10, RM	0/2	0/2
11, RM	0/2	0/2
12, RM	0/2	0/2
13, RM	0/2	0/2
14, RM	1/5	0/5
15, RM	0/2	0/2
16, cancer	0/1	0/1
17, cancer	0/1	0/1
18, cancer	0/1	0/1
19, cancer	0/1	0/1
20, cancer	0/1	0/1
21, cancer	0/1	0/1
22, cancer	0/1	0/1
23, cancer	0/1	0/1
24, cancer	0/2**	0/2**
25, cancer	0/2**	0/2**
26, cancer	0/2**	0/2**
27, cancer	2/2**	2/2**
28, cancer	0/2**	0/2**
29, cancer	0/2**	0/2**
30, cancer	0/2**	0/2**
Total	4/92	6/92

*Tissue was classified as derived from a cancer patient if ratio of concentrations (Fapy-A + Fapy-G)/(8-OH-Ade + 8-OH-Gua + HMUra) < 1.32 (second column) or (Fapy-A)/(8-OH-Gua) < 5.6 (third column).
**Represents paired IDC and MNT from the same patient.

The ratio of base lesions is a function of the redox environment of the DNA. Fapy derivatives predominate under reducing conditions, whereas 8-OH adducts are associated with oxidative conditions (12). Although both types of lesions are products of oxidative stress on the DNA, the greatest cancer threat is clearly related to 8-OH adduct formation. In fact, our current evidence suggests that Fapy structures have protective properties and that they are essential structural components of DNA in healthy breast tissues. Thus, the base lesion profiles provide a unique perspective of the redox potential of the cell, the oxidative status of the DNA, and the overall health of the tissues given that carcinogenesis is a product of oxidative stimulus.

As outlined below, there are substantial and diverse applications for the technical capabilities that formed the basis for a new perspective of cancer and its early prediction. The new perspective, which is consistent with Dr. Thorgeirsson's (17) editorial views, "may provide a powerful tool for clinical oncology and preventive medicine." Further, "new insights into the mechanism of human carcinogenesis may also be realized."

The substantial changes we observed in the DNA base structure between normal and neoplastic breast tissues suggests that these would induce local and global alterations in the classical perception of DNA structure and function --changes that involve molecular interactions that would be manifested through vibrational spectroscopy, such as Fourier transform-infrared (FT-IR) and Fourir transform Raman (FT-R) spectroscopy. In fact, major differences we observed in the spectra, notably intensities of bands at about 1240 cm^{-1} and 950 cm^{-1} representing substantial changes in interaction between the nucleotide bases and the phosphodiester backbone. These spectral changes indicated that the attack

of the •OH on the base structure of DNA in normal breast tissue had altered IR bands at the above wavelengths --that is, modified the vibrational properties of important functional groups in this biopolymer.

A Euclidean search (computer evaluation) of the spectral profiles revealed dramatic differences between the DNA from cancerous and non-cancerous breast tissue. The following important interpretation of the data was made on the basis of the GC-MS/SIM and FT-IR spectral findings: The Fapy derivatives in the normal breast DNA are a likely normal means of "trapping" OH derivatives in a non-genotoxic structure and this produces a "unique form" of DNA that is "destabilized" when a shift in the redox balance occurs in the cell favoring the formation of potentially mutagenic radical-induced OH-adducts. These changes observed in our studies provide a new and potentially rewarding framework for the prediction of cancer risk long before cancer cells are formed (Figure 2), and constitute the elements of a new paradigm for oncogenesis in the female breast and possibly in other cancer-prone tissues from humans and animals as well.

Figure 2. ***The predicted probability of the cancerous origin of a tissue plotted with log_{10}((Fapy-A + Fapy-G)/(8-OH-Ade + 8-OH-Gua))***

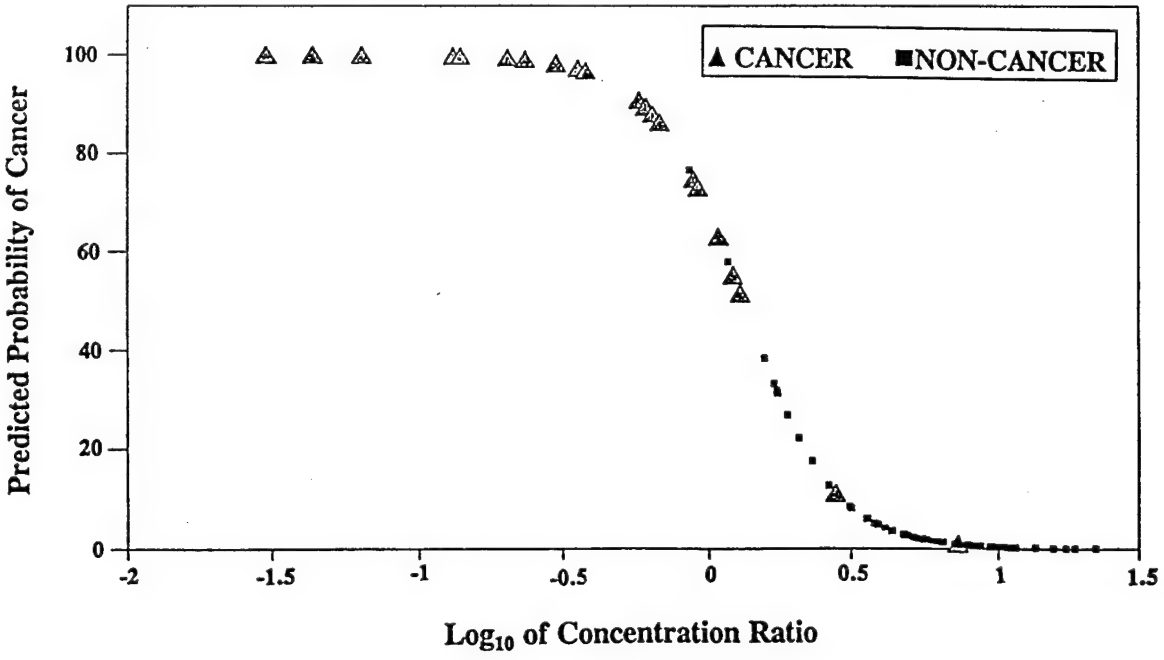

C. Purpose of the present work

In the one year period of this study, we have explored the use of FT-IR spectroscopy to supplement our understanding of breast cancer. Interpretation of data from a number of samples studied by FT-IR spectroscopy solidly indicate that this type of spectroscopy provides an exciting new dimension to our previously obtained nucleotide base data acquired by GC-MS/SIM. Moreover, a most important attribute of the FT-IR technique is that only a few micrograms (e.g., ~5 μg) of DNA are required; thus we believe that it is possible to obtain sufficient DNA from virtually any animal system, such as through a fine needle biopsy of the breast or the excision of a few micrograms of liver tissue from a Medaka exposed to environmental chemicals. Moreover, the FT-IR analysis of DNA takes less than 10 minutes, can be performed at a modest cost, and all data acquisition and processing is conducted using the instrument's software (e.g., the Euclidean Search program previously mentioned).

Another attractive analytical tool for identifying radical-induced base lesions in breast tissue involves monoclonal antibody technology. Previous studies (18-20) have indicated the strong potential of specific monoclonal antibodies for the detection and quantitation of modified DNA bases.

Previous reports of the production and application of monoclonal antibodies specific for modified DNA base structures have focused on, for example, methyl and acetyl derivatives of purines and pyrimidines (18) and etheno derivatives of guanosine (19). These adducts result from methylation or acetylation reactions with the DNA or arise as a consequence of a reaction with vinyl chloride or one of its metabolites. In

addition, Park et al. (20) reported the production of a monoclonal antibody reactive with 8-OH-Gua and its application to the study of 8-OH-Gua in biological fluids. Despite the close structural similarity to the respective unmodified base in these instances, the antibodies produced were of very high specificity, suitable for the establishment of immunoassays with limits of detection of modified bases in the 50 to 350 fmol/assay range. This is similar to the range of detectability currently found with GC-MS/SIM analyses of oxidized bases. Thus, it is highly likely that a simple, rapid, and convenient monoclonal antibody-based immunoassay method could be established for the detection and quantitation of Fapy and 8-OH adducts of purines resulting from •OH-induced base damage to the DNA.

II. BODY

A. Methods Used

1. Acquisition of tissues

The livers from fish were excised and the DNA was extracted as previously reported (9). RMT was obtained randomly from patients residing in the Puget Sound region of Washington State. In addition, tumor tissues, IDC and MNT specimens were obtained from the breasts of surgical patients. The IDC and MNT specimens were obtained from local hospitals and The Cooperative Human Tissue Network (Cleveland, OH). The RMT and the MNT exhibited occasional incidences of nonneoplastic fibrocystic changes; other cellular changes were essentially absent.

2. GC-MS analysis

After excision, the tissue was immediately frozen in liquid nitrogen and maintained at ~70°C. The frozen tissue (20 - 350 mg, depending on the DNA content) was minced with a scalpel, placed in 3 ml of phosphate buffer solution and homogenized for one minute over ice. Then 2.0 ml of 2X Lysis buffer (Applied Biosystems, Inc., Foster City, CA) and 300 μL of RNase A (Boehringer-Mannheim, Corp., Indianapolis, IN) were added and the sample was incubated at 60°C for one hour. Proteinase K (Applied Biosystems, Inc.) was added and incubation was allowed to proceed overnight at 60°C. DNA was then extracted as previously described (12). The DNA was hydrolyzed using 60% formic acid, which does not result in significant oxidation of the nucleotide bases (16, 21). Trimethylsilyl (TMS) derivatives of the previously determined nucleotide bases (21) were analyzed by gas chromatography-mass spectrometry with selected ion monitoring (GC-MS/SIM) (8-13) using a Hewlett-Packard Model 5890 microprocessor-controlled gas chromatograph interfaced to a Hewlett-Packard Model 5970B mass selective detector. The injector port and interface were both maintained at 260°C. The column was a fused silica capillary column (12.0 m; 0.2 mm inner diameter) coated with cross-linked 5% phenylmethyl-silicone gum phase (film thickness, 0.33 μm). The column temperature was increased from 120°C to 235°C at 10°C/min. after initially being held for 2 min. at 120°C. Helium was used as the carrier gas with a flow of 1.0 ml/min through the column. The amount of TMS hydrolysate injected onto the column was 0.5 μg. Quantitation of the DNA lesions was undertaken on the basis of the principal ion and confirmation of structure was undertaken by using qualifier ions. For example, the primary ion for the

TMS derivative of Fapy-A was m/z = 354 and the main qualifier ion was m/z = 369 (21). All analyses were performed in duplicate or triplicate, depending on the amount of tissue available and the lipid content. Reproducibility between determinations was greater than 90%. Calf thymus DNA was used as a negative control and showed minimal DNA base lesions (concentrations close to those at the threshold of detection for the GC-MS/SIM procedure) (10).

Calf thymus DNA, used as a representative normal tissue, Fapy-A and the pyrimidine base, HMUra, were purchased from Sigma Chemical Co., and 8-OH-Gua was obtained from the Chemical Dynamics Corp. The 8-OH-Ade and Fapy-G were synthesized and purified in our laboratories as previously described (10).

3. FT-IR analysis

The DNA for FT-IR analysis, dissolved in deionized water, was aliquoted into portions (~ 20 μg). The aliquots were dried completely by lyophilization, purged with pure nitrogen and stored in an evacuated, sealed glass vial.

Spectra of DNA samples were obtained with a Perkin-Elmer System 2000 Fourier Transform-IR spectrometer (The Perkin-Elmer Corp., Norwalk, CT) equipped with an IR microscope and a wide range mercury-cadmium-telluride detector. The DNA was placed on a BaF_2 plate in an atmosphere with a relative humidity of less than ~60% and flattened to make a transparent film. Using the IR microscope in a visual observation mode, a uniform and transparent portion of the sample was selected to avoid a scattering or wedge effect in obtaining transmission spectra. Each analysis was performed in triplicate on

~5μg of DNA and the spectra were computer averaged. Two hundred and fifty-six scans at 4 cm^{-1} resolution were performed for each analysis to obtain spectra in a frequency range of 4000-700 cm^{-1}. Typically 3-5 minutes elapsed from when the glass vial was broken to when each IR spectrum was obtained. None of the IR spectra showed a 1703 cm^{-1} band, which is indicative of specific base pairing. This fact indicates that the samples were essentially free from water.

The IR spectra were obtained in transmission units and converted to absorbance units for data processing. The Infrared Data Manager software package (The Perkin-Elmer Corp.) was used to control the spectrometer, to obtain the IR spectra, deconvolute the spectra and to perform the Euclidean Distance analysis of spectra. Deconvolution was achieved using a width factor of 42.0 and a smoothing factor of 30.0 on all the spectra.

The GRAMS/2000 software package (Galactic Industries Corp., Salem, NH) was also used to perform post-run spectrographic data analysis. Each spectrum was converted to a spreadsheet format giving a specific absorbance for every wavenumber between 4000 and 700 cm^{-1}.

4. Monoclonal Antibodies

a. Preparation of Immunogens.

The oxidized nucleosides 8-OH-Ade and 8-OH-Gua were prepared as previously described (10). Coupling of haptens to carrier protein were conducted through the ribose moiety of the nucleoside after oxidization by $NaIO_4$. The antigen for immunization was prepared by Schiff base formation with lysine groups of keyhole limpet hemocyanin

followed by reduction with $NaCNBH_3$. Similar hapten-BSA conjugates were prepared for screening.

b. Preparation and screening of monoclonal antibodies.

Balb/c mice were injected subcutaneously at 10 day intervals (50 μl each, 0.5 μg/μl conjugate) prepared as a suspension in monophosphoryl lipid A plus trihalose dimycolate adjuvant. Spleen cells were isolated and fused with mouse X63 myeloma cells. Culture supernatant were tested for binding to hapten conjugated BSA in a solid phase binding assay (see below). Wells containing reactive antibodies were moved to 24-well plates and expanded for more detailed analysis of binding specificity. Each reactive antibody was tested for specificity by comparison of reactivity with BSA conjugates linked to the specific antigen, native base structure, and negative control. Wells showing antibody of proper specificity were selected and cloned to yield a monoclonal antibody producing cell line.

c. Solid phase antibody screening assays.

Hapten-conjugated BSA is coated on 96-well Falcon Pro-bind plated using 50 μg protein per ml of 50 mM sodium phosphate buffer, pH 7.5, 5 mM $MgCl_2$, 15 mM NaN_3 in an overnight incubation. The plates were blocked with PBS containing 5% BSA followed by incubation with culture supernatant for 18 hours. The plates were washed with PBS followed by incubation with 1:500 diluted rabbit anti-mouse whole Ig (ICN Immunobiologicals) for 1 hour. The plates were again washed with PBS and incubated

with ^{125}I-protein A (90,000 cpm/well) for 1 hour. The plates were washed again with PBS and the amount of ^{125}I in each well was determined in a gamma counter.

d. Detailed antibody characterization.

Antigen binding constants were determined in radioimmunoassays with the specific antigen to determine the constants for each antibody. Further, competitive RIA's were conducted with a variety of nucleotide bases and base derivatives to determine inhibition constants for binding to the specific antigen. Those antibodies showing the highest specificity and capable of detecting the lowest quantity of antigen were used further.

B. Results

1. GC-MS and FT-IR results

The GC-MS/SIM analyses showed that the mean values for the base lesions (Fapy-A, 8-OH-Ade, Fapy-G and 8-OH-Gua) in the normal and cancer tissues were consistent with previous data found in this laboratory (12).

FT-IR spectroscopy revealed remarkable structural differences in the cancer and noncancer tissues. The ages of the patients with and without cancer differed (the patients with cancer were on average approximately 16 years older than those without cancer; 56 vs. 40 years); however, none of the spectral characteristics that had statistically significant associations with cancer/noncancer status had a statistically significant association with age.

The main features of the spectral profiles resemble those of DNA from normal tissues obtained previously in studies using IR spectroscopy (22), as outlined in Table 3.

For example, the area 1700 to 1500-cm^{-1} was assigned to strong CO stretching and NH_2 bending vibrations, and 1550-1300 cm^{-1} was assigned to weak NH vibrations and CH in-plane base deformations; 1240 cm^{-1} represents medium PO_2 antisymmetric-stretching vibrations of the phosphodiester backbone; 1100 to 900 cm^{-1} represents strong PO_2-symmetric stretching vibrations (~1080 cm^{-1}), the CO-stretching vibrations of the deoxyribose moiety and the PO-stretching vibrations of the PO group of the phosphodiester backbone.

Table 3. ***Assignment of DNA absorption bands***

Wavenumber (cm^{-1})	Assignment	Notes
1700 - 1500 s	CO stretching, NH_2 bending	paired (G-C, A-T) and unpaired bases
1500 - 1300 w	NH, CH in-plane base deformations	
1240 m	PO_2 antisymmetric stretching	weak CC, CN bands nearby
1100 - 900 s	PO_2 symmetric stretching at 1080 cm^{-1} CO stretching of deoxyribose PO stretching of phosphodiester group	

(s = strong; m = medium; w = weak)

The mean spectra of the cancer and noncancer tissues are shown in Figure 3. The spectra were not uniform in the occurrence of cancer and noncancer differences. Areas in which cancer and noncancer spectra were notably different include approximately the 1720-, 1170-, 1070-, 1030-, 940-, 860- and 790-cm^{-1} areas. It is notable that the noncancer spectra were more diverse than the cancer spectra and generally more dissimilar.

Figure 3. ***Mean spectra (deconvoluted) of the cancer and noncancer tissues***

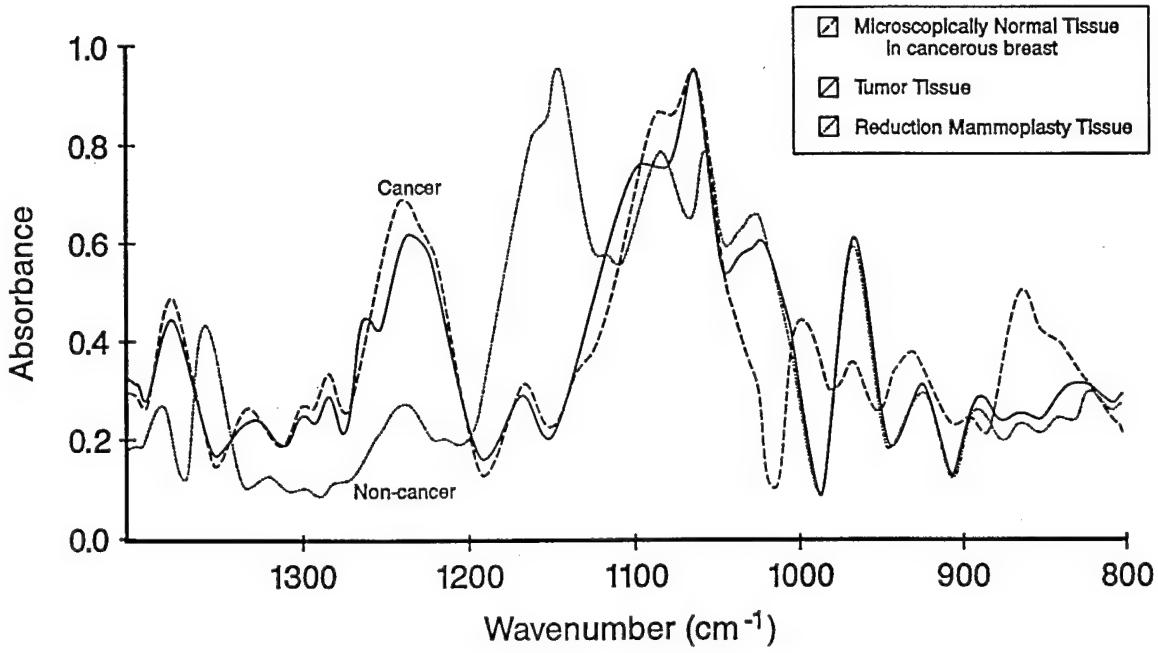

Shifts in the Spectra Toward a Cancer-like Phenotype

The cancer spectra were taken as a reference library. The closeness or distance of each noncancer spectrum from the cancer library was measured by a Euclidean Search. This measures the correlation coefficient between the index spectrum and the spectrum of each member of the cancer library, producing a number of correlations. For each spectrum, these correlations were averaged to produce a single mean Euclidean Search correlation (Figure 4). Quite surprisingly, the correlations were widespread (ranging from 0.2 to 0.88) among the noncancer tissues and could be grouped quite easily. We chose to

designate three groups and labeled them "low," medium," and "high" to indicate their correlation with (or distance from)the cancer library.

Figure 4. ***Mean Euclidean Search correlation values for noncancer tissues***

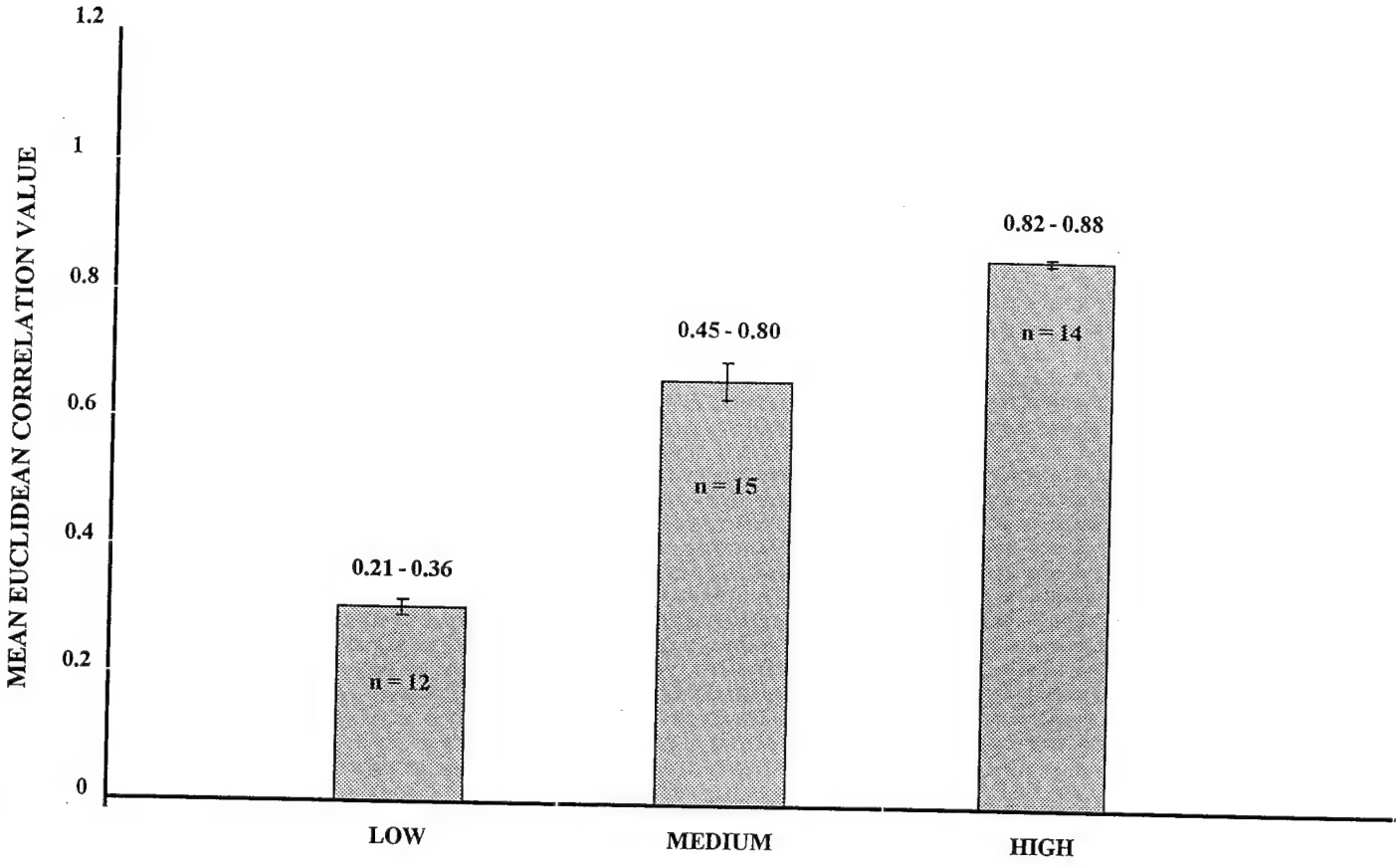

Relationship of Spectral Features to Base Modifications

Some of our spectral descriptive measures were related to the Fapy-A/8-OH-Ade base model, developed previously (12; Figure 5). The logarithm of the ratio of base concentrations was correlated significantly with several of the spectral descriptive measures as shown in Table 4. This analysis has reduced significance compared to analyses based solely on spectral data because of the smaller number of patients with GC-

MS data. Still, several of the correlations were statistically significant or had correlations of ±0.3 or larger. These correlations of independently derived spectral measures with a GC-MS-based measure of cancer risk mutually support the finding that both approaches are able to discriminate between patients with and without cancer and establish potential cancer risk levels.

Figure 5. ***Mean log_{10} Euclidean Search correlation profile compared to mean log_{10}(Fapy-A/8-OH-Ade)***

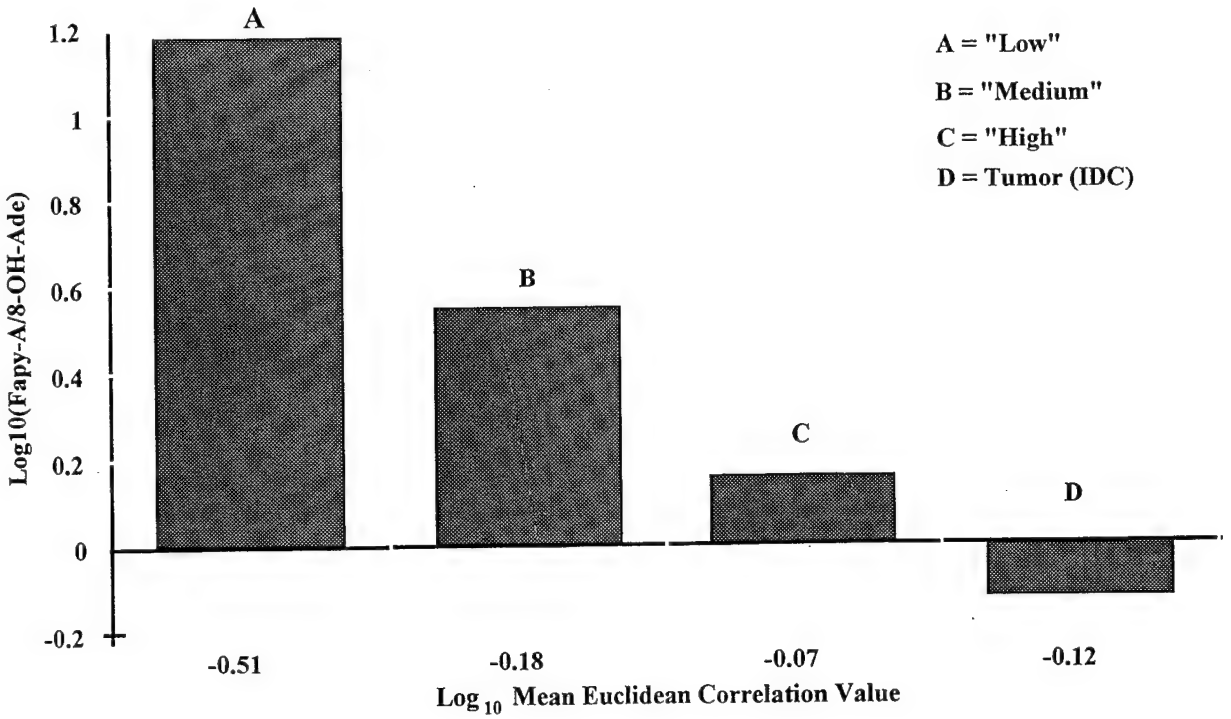

Table 4. Comparison of spectral descriptive characteristics for cancer (n=18) and noncancer (n=29) patients.

Item	Cancer mean (±SD)	Noncancer mean (±SD)	P-value
Distance C: Mean Pearson correlation with cancer library for 1503-761 cm^{-1}	0.93 (±0.03)	0.87 (±0.10)	0.003*†
Distance A: "airline distance" from cancer library for 1503-761 cm^{-1}	5.4 (±0.8)	7.7 (±3.6)	0.01†
Peak intensities and wavenumber location			
peak "A" in 1652 cm^{-1} area			
normalized absorbance	2.4 (±0.5)	2.3 (±0.5)	0.6
location (cm^{-1})	1652 (±6)	1652 (±7)	0.9
peak "B" in 1410 cm^{-1} area			
normalized absorbance	1.1 (±0.2)	1.2 (±0.3)	0.4
location (cm^{-1})	1412 (±6)	1407 (±10)	0.02†
peak "C" in 1233 cm^{-1} area			
normalized absorbance	1.3 (±0.2)	1.2 (±0.3)	0.09
location (cm^{-1})	1232 (±7)	1235 (±7)	0.1
peak "D" in 1061 cm^{-1} area			
normalized absorbance	2.4 (±0.2)	2.3 (±0.3)	0.1†
location (cm^{-1})	1060 (±6)	1062 (±13)	0.4†
log_{10} (Fapy-A/8-OH-Ade)	-0.31 (±0.35) (n=10)	0.39 (±0.61) (n=19)	0.001†

SD: standard deviation

* P-value based on permutation test is 0.004.

† t-test based on unequal variances.

3. Monoclonal Antibody Studies

a. Using the methodology described under "Methods" we have produced adequate amounts of highly purified 8-OH-adenosine and 8-OH-guanosine from their respective 8-Br-precursors (Table 5). Both compounds have been subjected to GC-MS/SIM analysis and shown to be of >99% purity.

Table 5. ***Summary of 8-OH-Adenosine fusions***

	# Positive Wells	#Specific Wells
Fusion 1 (Protocol 1)	79	23
Fusion 2 (Protocol 2)	96 (212)	38

The resulting oxidized nucleotide was further oxidized with $NaIO_4$ yielding a dialdehyde derivative of ribose capable of forming a Schiff base intermediate with a primary amino group. Reduction of the Schiff base with $NaCNBH_3$ provided a stable product in which the oxidized nucleotide hapten was coupled to either keyhole limpet hemocyanin for use as an immunogen or BSA for antibody screening. Mice were immunized with hapten conjugated keyhole limpet hemocyanin using a standard protocol and spleen cells were then fused with myeloma cells. After fusion of spleen cells with myeloma cells, the resulting hybridomas were screened with hapten conjugated BSA coated on plastic plates.

Fusions have been done with 8-OH-adenosine conjugates and we have generated 61 independent hybridoma clones specifically reactive with 8-OH-adenosine and not adenosine. Of these 61, four have been cloned into monoclonal antibody producing cell lines, each expressing independent antibodies of the IgG_1 isotype.

Each of these four antibodies has near absolute specificity for 8-OH-Ade with negligible reactivity with adenosine above background. These antibodies, demonstrate the ability of monoclonal antibodies reactive to oxidized nucleotide base structures to discriminate with high sensitivity and specificity subtle properties of appropriate antigens. These antibodies are applicable for the analysis of these antigens in more complex mixtures.

Similar studies were conducted with conjugates of 8-OH-guanosine. Highly purified antigen has been prepared and mice were immunized with the KLH conjugate prior to fusion and hybridoma production.

As shown in Figure 6, each of these 4 antibodies so far cloned has near absolute specificity for 8-OH-Ade with negligible reactivity with Ade above background. These antibodies demonstrate the ability of monoclonal antibodies reactive to oxidized nucleotide base structures to discriminate with high sensitivity and specificity subtle properties of appropriate antigens. These antibodies are applicable for the analysis of these antigens in more complex mixtures. Thus, there is strong probability for the success of this approach for the analysis and measurement of oxidative lesions in the bases of DNA as described.

Figure 6. ***Solid phase immunoassay of anti-8-OH-Adenosine monoclonal antibodies***

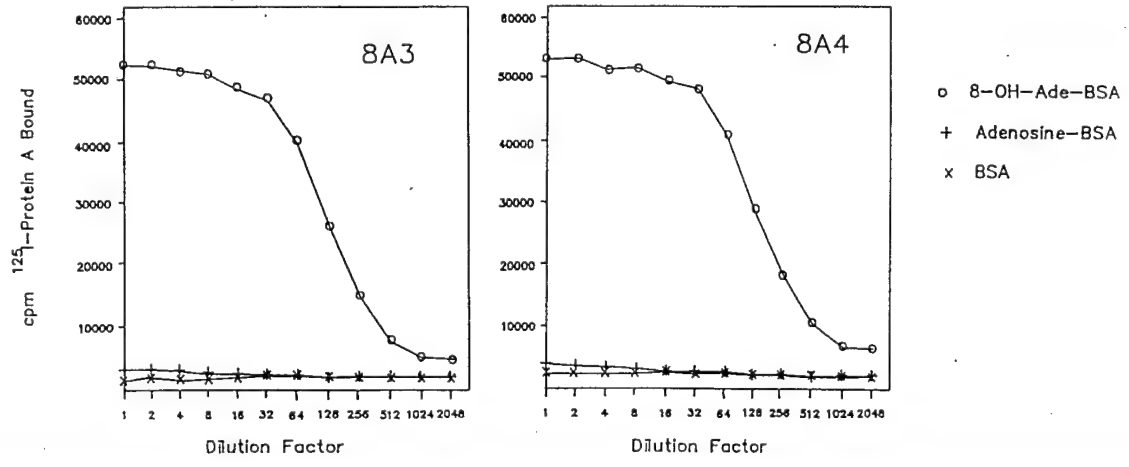

C. Discussion

The results describe the ability of FT-IR spectroscopy to discriminate cancer versus noncancer status based on differences in intrinsic chemical properties of DNA. The region of the IR spectrum associated with vibrational transitions of structural substituents of nucleotide bases, deoxyribose and phosphodiester moieties defines the most strikingly consistent, nonrandom differences between the cancer and noncancer groups. Thus, the nonrandom variation found most likely was due to inherent chemical properties that are characteristic of each group.

The spectral profiles obtained in the present study appear to reflect considerable differences in the modification of the nucleotide bases, phosphodiester groups and the deoxyribose moiety between cancer and noncancer groups relative to the attack of the •OH on DNA. However, other reactions cannot be ruled out. Difficulties presently exist in precisely defining the proportions of damage inflicted on any of these structural components or to specifically identify the exact nature of the functional groups involved. A clearer understanding of these important issues will require detailed study in the future using, for example, oligonucleotides containing known types and amounts of base lesions. Nevertheless, it has been shown that the •OH attacks the deoxyribose moiety to produce a variety of products resulting from hydrogen abstractions of the pentose ring (23). These reactions result in ring-opening products and the formation of a carbon centered radical at the 5′carbon position, linking deoxyribose residues with the phosphodiester groups. The attack of the •OH on the deoxyribose moiety is known to result ultimately in strand

breakage (23). In this regard, the damage inflicted on the DNA from the normal and cancer tissue was broadly different.

Major alterations in the DNA bases are attributed to reactions involving the •OH (11), which may arise from H_2O_2 via the Fe^{++}-catalyzed Fenton reaction (5). The H_2O_2 is possibly produced through the redox cycling (24) of a number of the environmental chemicals to which the fish were continually exposed. The initial attack of the •OH probably first involves the formation of the 8-oxyl derivatives of adenine ($A8OH^{\bullet}$) and guanine ($G8OH^{\bullet}$) 8, 12). At this point, the cellular redox status appears to be critical in determining the degree to which ring-opening products vs. 8-OH-adducts are formed (8, 12). Given that recent evidence indicates that the reductively formed Fapy derivatives block DNA replication (2) and mRNA transcription (25), whereas at least 8-OH-Gua leads to a significant base misreading (15), exposed animals and humans would be expected to have a significant advantage in avoiding cancer by favoring the reductive (Fapy) pathway. In addition, high concentrations of Fapy derivatives in the DNA of tissues are likely to slow DNA replication, thereby enhancing the surveillance and repair of OH-adducts during cell division (8, 12). Accordingly, 8-OH-Gua may have a diminished genotoxicity in the presence of the elevated concentrations of Fapy derivatives.

The importance of the Fapy derivatives in carcinogenesis is only just being recognized (12). High concentrations of Fapy-G were also found in the cancerous livers of English sole exposed to hydrocarbons (11). Also, as indicated, high ratios of Fapy-A to 8-OH-Gua and 8-OH-Ade were shown to occur in the healthy female breast (12). Fapy-A was substantially depleted, however, in the cancerous breast in favor of the 8-OH-adducts.

Thus, the putative role played by the Fapy derivatives in protecting tissues against the carcinogenic effects of mutagenic base products (8, 12) may well be phylogenetically conserved.

The reaction of the •OH with DNA is known to involve the modification of diverse structural groups. Previous studies with *in vitro* systems (23) have shown that the •OH attacks the deoxyribose moiety giving rise to a variety of products resulting from hydrogen abstractions of the pentose ring. These lead to ring-opening structures and a carbon centered radical at the 5' carbon which links the deoxyribose moiety with the phosphodiester group. A number of radical intermediates are formed which ultimately result in the loss of phosphoric acid and strand breakage (23).

FT-IR spectroscopy of control DNA and that of the exposed groups provided the first direct evidence in a living system for profound chemically-induced damage to the infrastructure of this biopolymer, as exemplified by the fact that a high proportion of the spectral difference between 1500 and 700 cm^{-1} was statistically significant (Fig. 3). It is not possible to attribute all of this damage to the action of the •OH; however, at least the substantial alterations in the NH and CO vibrations of the nucleotide bases and the deoxyribose moiety were likely associated with this highly reactive oxygen species.

The introduction of potentially mutagenic base alterations, such as 8-OH-Gua, into the DNA was substantial and would likely increase the cancer risk. This may be partly due to the fact that the replacement of 8-OH-Gua for guanine in DNA profoundly inhibits the methylation of cytosines controlling gene expression (26).

Almost certainly, the xenobiotic-induced DNA damage found in the present work created a considerable degree of genetic instability. This may well be pivotal in the activation of oncogenes and the deregulation of tumor suppressor genes, such as p53 (28), and it may at least partially explain the timing of oncogenesis and the timate manifestation of cancer. In this regard, the findings provide an important framework for future studies, with a variety of chemically-stressed biological systems, to better understand the nature of the presently reported structural changes in DNA and their implications to carcinogenesis.

An indication of the spectral distinctions that can be made between Medaka exposed to water-borne trichloroethylene at Fort Detrick and unexposed controls is given in Figure 7.

Figure 7. ***Deconvoluted spectra of control and test medaka liver***

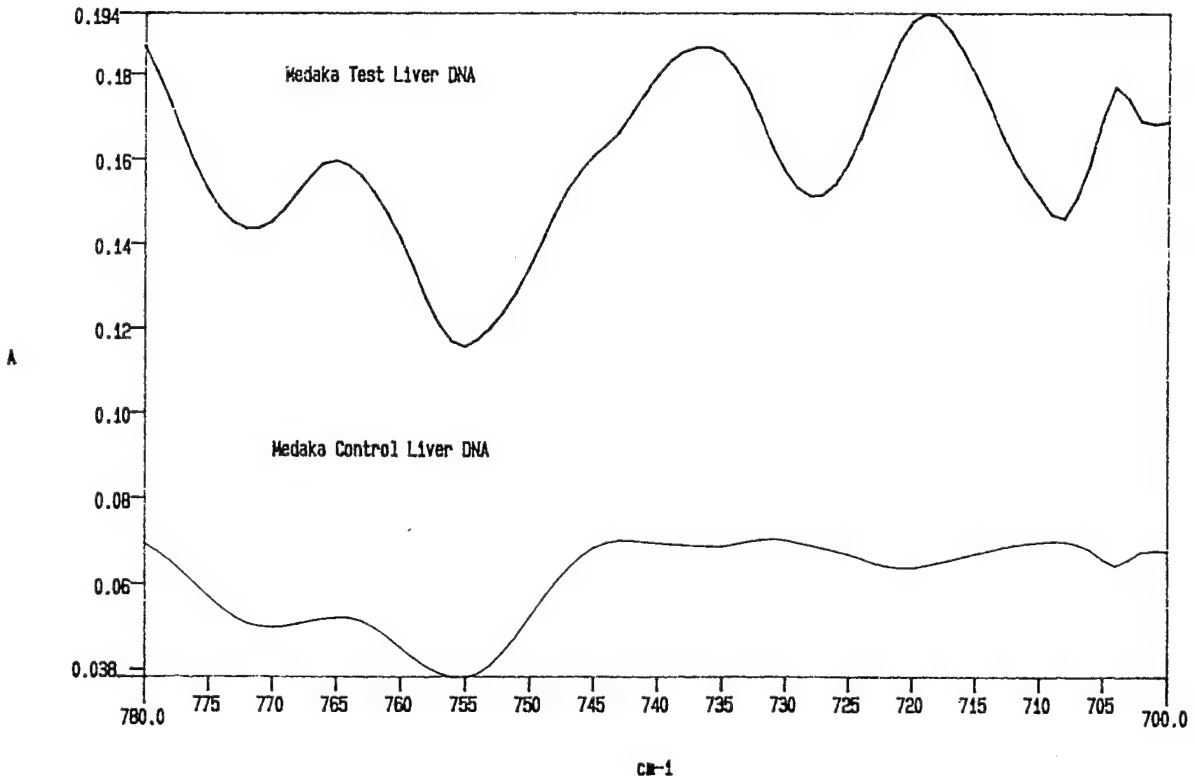

An additional example of spectral distinctions, based on a Euclidean search analysis of DNA from three groups of normal breast tissues are presented in Figure 8. The projected "risk"(low, medium and high) is based on the Euclidean distance from the tumor library (see figures 4 and 5).

Figure 8. ***Deconvoluted spectra of low, medium and high risk DNA compared to cancer DNA***

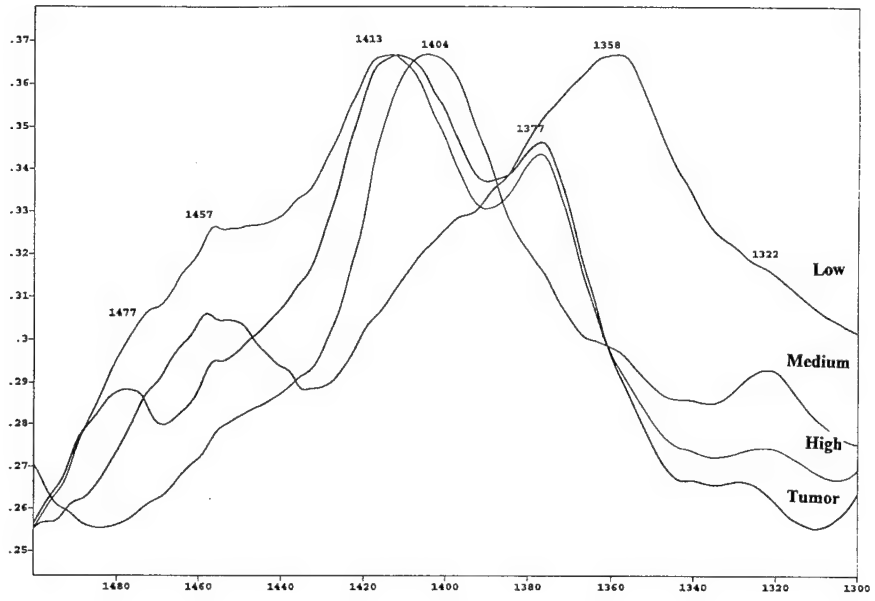

III. CONCLUSIONS

A. Implications of this work

1. FT-IR and GC-MS/SIM

The development of cancer is likely associated with increased exposure to materials capable of eliciting a mutagenic response and/or dietary deficiencies in protecting against oxidative damage. Given that carcinogenesis is a chronic process driven by an accumulation of random mutational events, that often develop over a number of years, it is

expected that a relatively high proportion of animal and human populations show evidence of premalignant changes in the DNA, as found in this report. However, it is expected that only a portion of those individuals, depending on their specific genetic susceptibilities and DNA lesion profiles, would achieve the necessary conditions leading to malignant conversion and tumorigenesis. Therefore, animal and human populations residing in areas with variable incidences of cancer likely have proportionate differences in the percentage of individuals having premalignant DNA changes of the type described.

The fact that the DNA underwent an unprecedented degree of structural modification suggests that it is considerably more responsive to oxidative stresses than previously believed possible. Accordingly, special importance is attached to reactions involving the •OH and possibly other reactive oxygen species in these structural modifications. Further, the diverse structural changes in the DNA, which are readily determined by FT-IR spectroscopy and GC-MS/SIM using small amounts of tissue, provide a promising new basis for the development of sensitive biomarkers for assessing genotoxic injury and cancer risk in human and animal populations.

2. Monoclonal Antibody Studies

The results demonstrate the high immunogenicity of oxidized base lesions that are the focus of the study. In one completed case we have obtained a significant number of independent hybridoma cell lines. The results suggest that these antibodies are capable of detecting specific antigen in an assay at the high 10's to low 100's of fmol per assay. These results offer high promise that a quantitative immunoassay for oxidative lesions of

purine bases is possible. Further studies are warranted to continue antibody production of Fapy base lesions and to formulate a protocol for quantitative determination of oxidized base lesions in DNA of organisms from a variety of exposure conditions for comparison with results from GC-MS/SIM and FT-IR analyses.

B. Nature of future work

Future work envisioned on the basis of the present findings relates to the development of cancer predictive models formulated from FT-IR and GC-MS data. These findings should include data from divergent species and tissues to verify the hypothesis that the spectral data is reflective of phylogenetically conserved processes--that is, that the analysis of DNA and the establishment of predictive models is not essentially dependent on the species or the tissue examined. Clearly, prospective studies are essential to ultimately test the validity of the predictive models on animal and human populations. In addition, this technology would be highly applicable to the introduction of a quantitative immunoassay for the DNA base lesions. This would involve further work on the use of monoclonal antibodies.

IV. REFERENCES

1. Springer D, Mahlum D, Westerburg K, Hopkins M, Frazier D, Later D, et al. Carcinogenesis, metabolism and DNA binding studies of complex organic mixtures. In: Cooke M, Dennis AJ, editors. Polynuclear Aromatic Hydrocarbons: Chemistry, Characterization and Carcinogenesis. Columbus: Battelle, 1986:881-92.

2. Klein JC, Bleeker MJ, Saris CP, Roelen HCPF, Brugghe HF, Van den Elst H, et al.. Repair and replication of plasmids with site-specific 8-oxodG and 8-AAFdG residues in normal and repair-deficient human cells. *Nucleic Acids Res* 1992; 20:4437-43.

3. Fraga CG, Shigenga MK, Park JW, Degan P and Ames BN. Oxidative damage to DNA during aging: 8-hydroxy-2'-deoxyguanosine in rat organ DNA and urine. *Proc. Natl. Acad. Sci. USA* 1990; 88:4690-4.

4. Zhao MJ, Jung L, Tanielian C, Mechin R. Kinetics of the competitive degradation of deoxyribose and other biomolecules by hydroxyl radicals produced by the Fenton reaction. *Free Radic Res* 1994; 20:345-63.

5. Imlay JA, Chin SM, Linn S.. Toxic DNA damage by hydrogen peroxide through the Fenton reaction *in vivo* and *in vitro*. *Science* 1988; 240:640-2.

6. Jernstrom B, Martinez M, Meyer DJ, Ketterer B. Glutathione conjugation of the carcinogenic and mutagenic electrophile (±)-7β,8α-dihydroxy-9α,10α-oxy-7,8,9,10-tetrahydrobenzo(*a*)pyrene catalyzed by purified rat liver glutathione transferase. *Carcinogenesis* 1985; 6:85-9.

7. Randerath E, Randerath K. Postlabeling methods - an historical review. *IARC Sci Publ* 1993; 124:305-14.

8. Malins DC, Ostrander GK, Haimanot R, Williams P. A novel DNA lesion in neoplastic livers of feral fish: 2,6-Diamino-4-hydroxy-5-formamidopyrimidine. *Carcinogenesis* 1990; 11:1045-7.

9. Malins DC, and Haimanot R. 4,6-Diamino-5-formamidopyrimidine, 8-hydroxyguanine and 8-hydroxyadenine in DNA from neoplastic liver of English sole exposed to carcinogens. *Biochem Biophys Res Commun* 1990; 173:614-9.

10. Malins DC, Haimanot R. Major alterations in the nucleotide structure of DNA in cancer of the female breast. *Cancer Res* 1991; 51:5430-2.

11. Malins DC, Haimanot R. The etiology of cancer: Hydroxyl radical-induced DNA lesions in histologically normal livers of fish from a population with liver tumors. *Aquatic Toxicology* 1991; 20:123-30.

12. Malins DC, Holmes EH, Polissar NL, Gunselman SJ. The etiology of breast cancer: characteristic alterations in hydroxyl radical-induced DNA base lesions during oncogenesis with potential for evaluating incidence risk. *Cancer* 1993; 71:3036-43.

13. Malins DC. Identification of hydroxyl radical-induced lesions in DNA base structure: Biomarkers with a putative link to cancer development. *J Toxicol Environ Health.* 1993; 40:247-61.

14. Floyd RA. The role of 8-hydroxyguanine in carcinogenesis. *Carcinogenesis* 1990; 11:1447-50.

15. Cheng KC, Cahill DS, Kasai H, Nishimura S, Loeb LA. 8-Hydroxyguanine, an abundant form of oxidative DNA damage, causes G→T and A→C substitutions. *J Biol Chem* 1992; 267:166-72.

16. Nackerdien Z, Olinski R, Dizdaroglu M. DNA base damage in chromatin of gamma-irradiated cultured human cells. *Free Radic Res Commun* 1992; 16:259-73.

17. Thorgeirsson SS. Endogenous DNA damage and breast cancer *Cancer* 1993; 71(10):2897-9.

18. Reynaud C, Bruno C, Boullanger P, Grange J, Barbesti S and Niveleau A. Monitoring of urinary excretion of modified nucleosides in cancer patients using a set of six monoclonal antibodies. *Cancer Lett* 1992; 61: 255-62.

19. Foiles PG, Miglietta LM, Nishikawa A, Kusmierek JT, Singer B and Chung FL. Development of monoclonal antibodies specific for 1,N^2-ethenodeoxyguanosine and N^2,3-ethenodeoxyguanosine and their use for quantitation of adducts in G12 cells exposed to chloroacetaldehyde. *Carcinogenesis* 1993; 14: 113-6.

20. Park EM, Shigenaga MK, Degan P, Korn TS, Kitzler JW, Wehr CM, Kolachana P and Ames BN. Assay of excised oxidative DNA lesions: Isolation of 8-oxoguanine and its nucleoside derivatives from biological fluids with a monoclonal antibody column. *Proc Natl Acad Sci USA* 1992; 89: 3375-9.

21. Dizdaroglu M. Application of capillary gas chromatography-mass spectrometry to chemical characterization of radiation-induced base damage of DNA: Implications for assessing DNA repair processes. *Anal. Biochem* 1985; 144:593-603.

22. Parker FS. Chapter 9. In: Applications of infrared, raman, and resonance raman spectroscopy in biochemistry. New York: Plenum, 1983:349-98.

23. Von Sonntag C, Hagen U, Schon-Bopp A, Schulte-Frohlinde D. Radiation-induced strand breaks in DNA: chemical and enzymatic analysis of end groups and mechanistic aspects. *Adv Radiat Biol* 1981; 9:109-42.

24. Roy D, Floyd RA and Liehr JG. Elevated 8-hydroxydeoxyguanosine levels in DNA of diethylstilbestrol-treated Syrian hamsters: covalent DNA damage by free radicals generated by redox cycling of diethylstilbestrol. *Cancer Res* 1991; 51: 3882-5.

25. Koch KS, Fletcher RG, Grond MP, Inyang AI, Lu XP, Brenner DA, et al. Inactivation of plasmid reporter gene expression by one benzo(a)pyrene diol-epoxide DNA adduct in adult rat hepatocytes. *Cancer Res* 1993; 53:2279-86.

26. Weitzman SA, Turk PW, Milkowski DH, Kozlowski K. Free radical adducts induce alterations in DNA cytosine methylation. *Proc Natl Acad Sci, USA* 1994; 91:1261-4.

27. Malins DC, McCain BB, Brown DW, Chan S-L, Meyers MS, Landahl JT, Prohaska PG, Friedman AJ, Rhodes LD, Burrows DG, Gronlund WD and Hodgins HO. Chemical pollutants in sediments and diseases of bottom-dweeling fish in Puget Sound, Washington. *Environ. Sci. Technol.* 1984; 18:705-13.

28. Hinds PW, Finlay CA, Quartin RS, Baker SJ, Fearon ER, Vogelstein B, et al. Mutant p53 DNA clones from human colon carcinomas cooperate with *ras* in

transforming primary rat cells: A comparison of the "hot spot" mutant phenotypes. *Cell Growth Differen* 1990; 1:571-80.

V. APPENDIX

A. DNA extraction yield of Medaka liver

MEDAKA LIVER TISSUES

Fish ID#	Mass of Liver (mg)	A260/280	DNA yield (ug)	
*EE3-93-027-15-1	1.8	1.3	40	
*EE3-93-027-15-2	3	0	0	
*EE3-93-027-15-3	5.9	1.31	1.31	
*EE3-93-027-15-4	2	0	0	
*EE3-93-027-15-5	2.8	0	0	
*EE3-93-027-15-6	1.2	0	0	
*EE3-93-027-15-7	2	1.32	22.25	
*EE3-93-027-15-8	0.7	1	0.15	
*EE3-93-027-15-9	2.3	1.26	3.15	
*EE3-93-027-15-10	3.3	1.24	2.85	
EE3-93-027-15-11	1.7	1.75	24.5	
EE3-93-027-15-12	3	2	1	
EE3-93-027-15-13	1.2	1.61	14.5	
EE3-93-027-15-14	4.9	1.97	67	
EE3-93-027-15-15	8.1	1.98	86	
EE3-93-027-15-16	1.9	1.66	74	
EE3-93-027-15-17	1.6	1.7	40	
EE3-93-027-15-18	0.9	1.71	18	
EE3-93-027-15-19	2.4	1.85	24	
EE3-93-027-15-20	3.1	1.67	40.5	
*EE3-93-027-15-21	2.4	1	19	
*EE3-93-027-15-22	0.2	0.96	48	
*EE3-93-027-15-23	1.4	1.04	39	
EE3-93-027-15-24	4.1	2.18	18.5	
EE3-93-027-15-25	2.4	2.17	13	
EE3-93-027-15-26	2.8	1.61	63	
*EE3-93-027-15-27	2.2	1.32	22.5	
*EE3-93-027-15-28	1.9	1.31	57	
EE3-93-027-15-29	4.5	1.6	30.5	
*EE3-93-027-15-30	2.5	1.37	98	
EE3-93-027-15-31	0.7	2.11	9.5	
EE3-93-027-15-32	3.6	2.2	11	
EE3-93-027-15-33	2.2	1.82	10	
EE3-93-027-15-34	1.9	1.73	9.5	
*EE3-93-027-15-35	1	1.32	16.5	
EE3-93-027-15-36	2.9	2.29	8	
*EE3-93-027-15-37	1.4	0	0	
*EE3-93-027-15-38	0.4	1.5	4.5	
*EE3-93-027-15-39	3.1	1.52	23.5	
EE3-93-027-15-40	0.9	1.9	27.5	
EE3-93-027-15-41	4.3	1.81	43.5	
*EE3-93-027-15-42	1.7	1.38	18	
EE3-93-027-15-43	3.6	1.86	41	
*EE3-93-027-15-44	2.5	1.28	18.5	
EE3-93-027-15-45	1.4	1.71	12	
*EE3-93-027-15-46	1.8	1.58	15	
EE3-93-027-15-47	2.9	1.7	17	
EE3-93-027-15-48	4	1.74	27	

MEDAKA LIVER TISSUES

Fish ID#	Mass of Liver (mg)	A260/280	DNA yield (ug)	
EE3-93-027-15-49	2.7	1.71	24	
EE3-93-027-15-50	1.7	1.85	12	
EE3-93-027-15-51	1.1	1.61	10.5	
EE3-93-027-15-52	0.6	1.64	9	
EE3-93-027-15-53	2.2	1.73	19	
EE3-93-027-15-54	2.7	1.84	17.5	
EE3-93-027-15-55	4.9	1.69	22	
EE3-93-027-15-56	2.1	1.73	13	
EE3-93-027-15-57	1.3	1.92	11.5	
EE3-93-027-15-58	1.8	1.81	14.5	
*EE3-93-027-15-59	2.8	1.33	84.5	
	2.63		25.24	

* NOT INCLUDED IN AVERAGES DUE TO FAILED EXTRACTION

Average liver mass = 2.63 mg
Average DNA recovery = 25.24 ug